NUMERICAL INVESTIGATION OF ELASTIC AND VISCOUS EFFECTS ON INERTIAL VISCOPLASTIC FLUID FLOWS

Daniel Dall'Onder dos Santos
Department of Mechanical Engineering, Federal University of Uberlândia, Av. João Naves de Ávila 2121, Uberlândia, MG, 38408-100, Brazil
dallonder@mecanica.ufu.br

Giovanni Minervino Furtado
Sérgio Frey
Department of Mechanical Engineering, Federal University of Rio Grande do Sul, Rua Sarmento Leite 425, Porto Alegre, RS, 90050-170, Brazil
giovannimf@mecanica.ufrgs.br
frey@mecanica.ufrgs.br

Mônica Feijó Naccache
Paulo Roberto de Souza Mendes
Department of Mechanical Engineering, Pontifícia Universidade Católica-RJ, Rua Marquês de São Vicente 225, Rio de Janeiro, RJ, 22453-900, Brazil
naccache@puc-rio.br
pmendes@puc-rio.br

Abstract. *From experimental observations, is known that some viscoplastic materials exhibit an elastic behavior when subjected to low shear rates. The main goal of this work is to perform numerical simulations of two-dimensional steady state laminar flows of elasto-viscoplastic fluids through a planar expansion-contraction. The mechanical model was defined by the mass conservation and momentum balance equations coupled to a new elasto-viscoplastic model. This modeling has been approximated by a stabilized multi-field finite element method based on the Galerkin least-squares methodology, having as primal variables the elastic extra-stress component, velocity and pressure fields. In this way, the compatibility conditions between the extra-stress-velocity and pressure-velocity finite element subspaces are violated, allowing to use equal-order finite element interpolations. The stabilized method has been implemented in the finite element code for non-Newtonian fluids under development at the Laboratory of Applied and Computational Fluid Mechanics (LAMAC) of the Federal University of Rio Grande do Sul. In the performed numerical simulations, the non-dimensional relaxation time, the jump number, the power-law coefficient, the non-dimensional flow rate and the non-dimensional density are varied in order to evaluate their influence on the elasto-viscoplastic fluid dynamics.*

Keywords: *elasto-viscoplastic flows, multi-field mechanical modeling, Galerkin least-squares, planar expansion-contraction flow*

1. INTRODUCTION

Non-Newtonian fluids are the majority of liquids found in nature and the study of their rheological behavior has a significant importance on different areas of engineering. Among them, there is a class of materials that exhibits little apparent deformation when subjected to a stress level behind an yield stress, referenced as viscoplastic liquids. Some of this materials also exhibit an elastic behavior at low shear rates, as is pointed out on several works in the literature – Carter and Warren, 1987, Beverly and Tanner, 1989, Mujumdar *et al.*, 2002, De Souza Mendes *et al.*, 2007, Sikorski *et al.*, 2009.

This work employs a model that best describes the actual flow of viscoplastic materials. For this issue, the mass conservation and momentum balance equations for incompressible fluids are coupled to a modification of the Oldroyd-B viscoelastic model. This modeling considers the material deforming with elasticity and high viscosity at low shear rates; on the vicinity of the yield stress, changes occur in the microstructure of the fluid and the viscosity decreases several orders of magnitude, the elasticity drops falls to very low values and the fluid begins to flow as pseudoplastic fluid.

The mechanical model mentioned above is approximated by a multi-field Galerkin least squares method, having as primal variables the extra stress, velocity and pressure fields. This methodology, introduced by Hughes *et al.*, 1986, for the Stokes problem, extended to the mixed Navier-Stokes formulations by Franca and Frey, 1992, and multi-fields by Behr *et al.*, 1993, does not neet the satisfy the compatibility conditions between the finite element sub-spaces for extra stress-velocity and pressure-velocity – also known as the Ladyzhenskaya-Babuška-Brezzi condition. It improves the stability of the classical Galerkin method adding mesh-dependent terms – functions of the residuals of the problem governing equations – evaluated on each element. As this residuals are trivially satisfied by the exact solution of the problem, the consistency is preserved in this class of methods.

The presented results aims the understanding of the flow dynamics of elasto-viscoplastic fluid flows through a planar expansion followed by a contraction. To pursue such a task, the following governing parameters are varied: the influence of the elasticity is obtained ranging the non-dimensional relaxation time θ_0^* from 0.75 to 25, the flow intensity effect ranging U^* from 0.01 to 1.0 and the inertia effect ranging the non-dimensionlal density ρ^* from 0 to 500.

2. THE MECHANICAL MODEL

The relevant equations for a multi-field boundary value problem accounting for isothermal and incompressible fluid flows may be formed by coupling the mass conservation and the momentum balance equations with the Oldroyd-B viscoelastic model. Subjecting the system to the appropriate velocity and stress boundary conditions and applying the elastic-viscous split stress (EVSS) scheme (Matallah *et al.*, 1998, Behr *et al.*, 2004, and references therein), it becomes

$$
\begin{aligned}
&\rho(\nabla\mathbf{u})\mathbf{u} = -\nabla p + \mathrm{div}\boldsymbol{\tau}_p + 2\eta_\infty(\dot\gamma)\mathrm{div}\mathbf{D}(\mathbf{u}) + \rho\mathbf{g} && \text{in } \Omega \\
&\boldsymbol{\tau}_p + \theta(\dot\gamma)\overset{\triangledown}{\boldsymbol{\tau}}_p = 2\eta_{eq}(\dot\gamma)\mathbf{D}(\mathbf{u}) && \text{in } \Omega \\
&\mathrm{div}\mathbf{u} = 0 && \text{in } \Omega \\
&\mathbf{u} = \mathbf{u}_g && \text{over } \Gamma_g^{\mathbf{u}} \\
&\boldsymbol{\tau}_p = \boldsymbol{\tau}_{pg} && \text{over } \Gamma_g^{\boldsymbol{\tau}_p} \\
&(-p\mathbf{I} + \boldsymbol{\tau})\mathbf{n} = \mathbf{t}_h && \text{over } \Gamma_h
\end{aligned}
\tag{1}
$$

where ρ is the fluid density, $\mathbf{u}$ the velocity vector, $\boldsymbol{\tau}_p$ the extra-stress tensor, $\mathbf{D}$ the strain rate tensor, p the hydrostatic pressure, $\mathbf{f}$ the body force vector; η_{eq} and θ_{eq} are, respectively, the viscosity and relaxation time for the fluid viscoelastic portion – functions of the second invariant of $\mathbf{D}$, η_∞ is the viscosity of the completely unstructured material, $\mathbf{t}_h$ is the stress vector, $\mathbf{u}_g$ and $\boldsymbol{\tau}_{pg}$ are the imposed velocity and extra-stress boundary conditions, respectively; $\overset{\triangledown}{\boldsymbol{\tau}}_p$ stands for the upper-convected time derivative of $\boldsymbol{\tau}_p$, given by

$$
\overset{\triangledown}{\boldsymbol{\tau}}_p = (\nabla\boldsymbol{\tau}_p)\mathbf{u} - (\nabla\mathbf{u})\boldsymbol{\tau}_p - \boldsymbol{\tau}_p(\nabla\mathbf{u}^T)
\tag{2}
$$

The elasto-viscoplastic model employed in this work is based on a modification of the viscosity function proposed by De Souza Mendes and Dutra, 2004, and the Oldroyd-B viscoelastic model, as mentioned before. The SMD modified viscosity function is given by

$$
\eta_{eq}(\dot\gamma) = \left(1 - \exp\left(-\frac{\eta_0}{\tau_0}\dot\gamma\right)\right)\left(\frac{\tau_0 - \tau_{0d}}{\dot\gamma}\exp\left(-\frac{\dot\gamma}{\dot\gamma_0}\right) + \frac{\tau_{0d}}{\dot\gamma} + K\dot\gamma^{n-1}\right) + \eta_\infty
\tag{3}
$$

where η_0 is the viscosity of the completely structured material, τ_0 is the static yield stress, τ_{0d} is the dynamic yield stress, $\dot\gamma_{0d}$ is the shear rate that marks the transition in the stress from τ_0 to τ_{0d}, K is the consistency index and n the power-law index – for more details, De Souza Mendes, 2009. The relaxation time θ_{eq} is defined as the relation between the purely viscous response of the material – given by the viscosity funtion on Eq. (3) – and the microstructure shear modulus G,

$$
\theta_{eq}(\dot\gamma) = \frac{\eta_{eq}(\dot\gamma)}{G(\lambda_{eq}(\dot\gamma))}
\tag{4}
$$

The expression employed to evaluate the microstructure shear modulus takes into account the the structure parameter λ_{eq}, also function of the strain rate, which measures the structuring level of the material. $G(\lambda_{eq})$ must be small when the fluid is fully structured ($\lambda_{eq} = 1$) and, on the limit where the structure is completely destroyed ($\lambda_{eq} = 0$), must tends to infinity to supress the elastic therm on Eq. (1b), describing in this way a purely viscous behavior. The expression employed to approximate this behavior is

$$
G = G_0 \exp\left(m\left(\frac{1}{\lambda_{eq}} - 1\right)\right)
\tag{5}
$$

where G_0 is the shear modulus of the completely structured material, m is a positive dimensionless constant and

$$
\lambda_{eq}(\dot\gamma) = \left(\frac{\ln\eta_{eq}(\dot\gamma) - \ln\eta_\infty}{\ln\eta_0 - \ln\eta_\infty}\right)
\tag{6}
$$

2.1 Dimensionless Parameters

The dimensionless parameters employed to characterize the flows are, firstly, the dimensionless flow rate U^*,

$$
U^* = \frac{u_c}{\dot\gamma_1 L_c}
\tag{7}
$$

where u_c is a characteristic velocity and L_c is a characteristic lenght, taken respectively as the channel inlet velocity and half of the entrance channel height; $\dot{\gamma}_1$ is defined as the strain rate where the fluid begins to flow as a power-law one ($\dot{\gamma}_1 = (\tau_{0d}/K)^{1/n}$) – see De Souza Mendes *et al.*, 2007, for more details. The viscosity jump when the stress is around the yield stress value is measured by the jump number J, and is written as

$$J = \frac{\eta_0 \dot{\gamma}_1}{\tau_0} - 1 \tag{8}$$

To quantify the elastic effects at the flow, its employed the non-dimensional relaxation time for the fully structures material, wich relates the microstructure shear modulus with the the static yield stress, $\theta_0^* = G_0/\tau_0$. The inertia effects are accounted by the non-dimensionlal density, given as

$$\rho^* = \frac{\rho(\dot{\gamma}_1 L_c)^2}{\tau_{0d}} \tag{9}$$

3. NUMERICAL APPROXIMATION

The Galerkin least-squares approximation for the boundary value problem defined on Eq. (1) can be written as: given the Dirichlet and Neumman boundary conditions, find the set $\boldsymbol{\tau}_p^h, \mathbf{u}^h, p^h \in \boldsymbol{\Sigma}^h \times \mathbf{V}^h \times P^h$ such that

$$B(\boldsymbol{\tau}_p^h, \mathbf{u}^h, p^h; \mathbf{S}^h, q^h, \mathbf{v}^h) = F(\mathbf{S}^h, q^h, \mathbf{v}^h) \, \forall \, (\mathbf{S}^h, q^h, \mathbf{v}^h) \in \boldsymbol{\Sigma}^h \times \mathbf{V}^h \times P^h \tag{10}$$

with

$$
\begin{aligned}
B(\boldsymbol{\tau}_p^h, \mathbf{u}^h, p^h; \mathbf{S}^h, \mathbf{v}^h, q^h) &= \int_\Omega \rho(\nabla \mathbf{u}^h)\mathbf{u}^h \cdot \mathbf{v}^h d\Omega \; - \int_\Omega p^h \mathrm{div}\mathbf{v}^h d\Omega \; + \int_\Omega \boldsymbol{\tau}_p^h \cdot \mathbf{D}(\mathbf{v}^h) d\Omega \\
&+ 2\eta_\infty \int_\Omega \mathbf{D}(\mathbf{u^h}) \cdot \mathbf{D}(\mathbf{v}^h) d\Omega \; + \int_\Omega \mathrm{div} \, \mathbf{u}^h q^h d\Omega \; + \epsilon \int_\Omega p^h q^h d\Omega \; + \int_\Omega \boldsymbol{\tau}_p^h \cdot \mathbf{S}^h d\Omega \\
&+ \int_\Omega \theta(\dot{\gamma}) \left([\nabla \boldsymbol{\tau}_p^h]\mathbf{u}^h \; - [\nabla \mathbf{u}^h]\boldsymbol{\tau}_p^h \; - \boldsymbol{\tau}_p^h[\nabla \mathbf{u}^h]^T\right) \cdot \mathbf{S}^h d\Omega \; - 2\eta_{eq}(\dot{\gamma}) \int_\Omega \mathbf{D}(\mathbf{u}^h) \cdot \mathbf{S}^h d\Omega \\
&+ \int_\Omega \mathrm{div} \, \mathbf{v}^h \delta(\mathrm{Re}_K) \, \mathrm{div} \, \mathbf{u}^h d\Omega \\
&+ \sum_{K \in \Omega^h} \int_{\Omega_K} \left(\rho(\nabla \mathbf{u}^h)\mathbf{u}^h + \nabla p^h - \mathrm{div} \, \boldsymbol{\tau}_p^h - 2\eta_\infty \, \mathrm{div} \, \mathbf{D}(\mathbf{u}^h)\right) \cdot \\
&\quad \cdot \alpha(\mathrm{Re}_K) \left(\rho(\nabla \mathbf{v}^h)\mathbf{u}^h + \nabla q^h - \mathrm{div} \, \mathbf{S}^h - 2\eta_\infty \, \mathrm{div} \, \mathbf{D}(\mathbf{v}^h)\right) d\Omega \\
&+ \beta \int_\Omega \left(\boldsymbol{\tau}_p^h + \theta(\dot{\gamma}) \left([\nabla \boldsymbol{\tau}_p^h]\mathbf{u}^h \; - [\nabla \mathbf{u}^h]\boldsymbol{\tau}_p^h \; - \boldsymbol{\tau}_p^h[\nabla \mathbf{u}^h]^T\right) - 2\eta_{eq}(\dot{\gamma})\mathbf{D}(\mathbf{u}^h)\right) \cdot \\
&\quad \cdot \left(\mathbf{S}^h + \theta(\dot{\gamma}) \left([\nabla \mathbf{S}^h]\mathbf{u}^h \; - [\nabla \mathbf{u}^h]\mathbf{S}^h \; - [\mathbf{S}^h](\nabla \mathbf{u}^h)^T\right) - 2\eta_{eq}(\dot{\gamma})\mathbf{D}(\mathbf{v}^h)\right) d\Omega
\end{aligned}
\tag{11}
$$

and

$$
\begin{aligned}
F(\mathbf{S}^h, \mathbf{v}^h, q^h) &= \int_\Omega \rho \mathbf{g} \cdot \mathbf{v}^h d\Omega + \int_{\Gamma_h} \mathbf{t}_h \cdot \mathbf{v}^h d\Gamma \\
&+ \sum_{K \in \Omega^h} \int_{\Omega_K} \rho \mathbf{g} \cdot \left(\alpha(\mathrm{Re}_K)(\rho(\nabla \mathbf{v}^h)\mathbf{u}^h + \nabla q^h - \mathrm{div} \, \mathbf{S}^h - 2\eta_\infty(\dot{\gamma})\mathrm{div}\mathbf{D}(\mathbf{v}^h))\right) d\Omega
\end{aligned}
\tag{12}
$$

D. Santos, G. Furtado, S. Frey, M. Naccache, P. de Souza Mendes
Numerical Investigation Of Elastic And Viscous Effects On Inertial Viscoplastic Fluid Flows

where $\epsilon << 1$ and β is a positive arbitrary value (Behr *et al.*, 1993); the mesh Reynolds number Re_K and the stability parameters $\alpha(\mathrm{Re}_K)$ and $\delta(\mathrm{Re}_K)$ are defined as in Franca and Frey, 1992, and Behr *et al.*, 1993,

$$\mathrm{Re}_K = \frac{\rho\, h_K\, \left|\mathbf{u}^h\right|_p m_k}{4\,\eta_{eq}(\dot{\gamma})}$$

$$\alpha(\mathrm{Re}_K) = \frac{h_K}{2\left|\mathbf{u}^h\right|_p \xi(\mathrm{Re}_K)} \quad , \quad \delta(\mathrm{Re}_K) = \lambda_d \left|\mathbf{u}^h\right|_p h_K \xi(\mathrm{Re}_K)$$

$$\xi(\mathrm{Re}_K) = \begin{cases} 0, & \text{if } 0 < \mathrm{Re}_K < 1 \\ 1, & \text{if } \mathrm{Re}_K \geq 1 \end{cases}$$

$$\left|\mathbf{u}^h\right|_p = \begin{cases} \left(\sum_{i=1}^{N} \left|\mathbf{u}^h\right|^p\right)^{1/p}, & \text{if } 1 \leq p < \infty \\ \max_{i=1,N} \left|u_i^h\right| \quad , & \text{if } p = \infty \end{cases}$$

$$m_k = \min\{1/3, 2C_k\}$$

$$C_k \sum_{K \in \Omega^h} h_K^2 \left\|\mathrm{div}\,\mathbf{S}^h\right\|_{0,K}^2 \geq \left\|\mathbf{S}^h\right\|_K^2 \quad \forall \;\; \mathbf{S}^h \in \mathbf{\Sigma}^h$$

(13)

where λ_d is a positive parameter and h_K is the mesh element size.

4. NUMERICAL RESULTS

Figure 1 shows a sketch of the analyzed geometry, a planar channel with a sudden expansion followed by a contraction. The employed boundary conditions to perform the numerical simulations are uniform parallel velocity u_0 at the channel inlet and outlet, no-slip and impermeability on channel walls and symmetry conditions along the channel centerline $(\partial_{x_2} u_1 = u_2 = \tau_{12} = 0)$. The expansion-contraction aspect ratios on height (H/h) and width (L/h) are set as 6.3. In order to guarantee fully-developed flow regions upstream and downstream channels, the mesh lengths either upstream or downstream of the expansion-contraction set equal to $20h$. After a mesh independence procedure that compares the transversal dimensionless stress profile at the expansion-contraction center for each consecutive mesh refinement, the selected mesh, with 5,200 bilinear Lagrangian (Q1) finite elements, presents an overall error less then 1% when compared to the next more refined mesh. A detail of the central portion of the employed mesh is depicted on Fig. 2. It's important mentioning that in all simulations performed in this work, $\eta_\infty \dot{\gamma}_1/\tau_{0d} = 10^{-2}$, $\dot{\gamma}_{0d}/\dot{\gamma}_1 = 10^{-4}$, $\tau_0/\tau_{0d} = 2$ and $m = 2$.
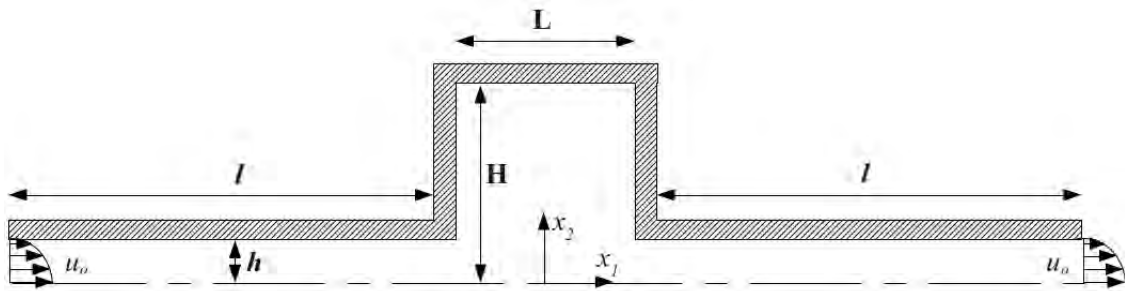

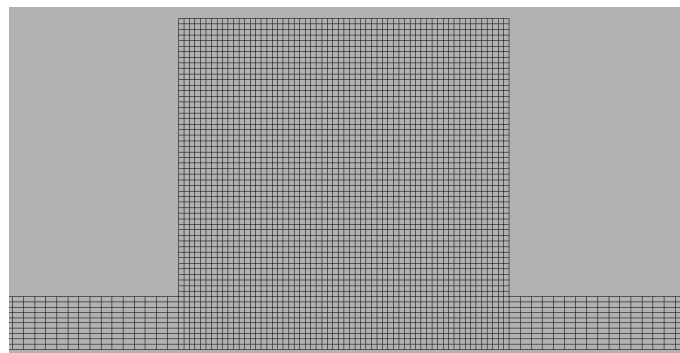Figure 1. Geometry and boundary conditions.

Figure 2. The central portion of the employed mesh.

An initial note must be made about the flow yield surfaces, which are usually defined as the surface where $\tau = \tau_0$. However, as $\dot{\gamma}$ varies some orders of magnitude with τ on the vicinity of $\tau = \tau_0$, this criterion may be inaccurate, once is susceptible to spurious oscillations. A more precise option is to defined the yield surfaces as the locus of points where $\dot{\gamma} = \dot{\gamma}_0$, with $\dot{\gamma}_0 = \tau_0/\eta_0$ – see Santos *et al.*, 2011, for details. Another important remark is about the elastic strain tensor field. The extra-stress tensor $\boldsymbol{\tau}$ is decomposed on two additive terms, namely a viscous one equal to $2\eta_\infty \mathbf{D}$ and a viscoelastic term $\boldsymbol{\tau}_p$ that obeys the Upper Convected Maxwell like differential equation – as pointed out previously by Eq. (1). The elastic strain tensor field is obtained dividing $\boldsymbol{\tau}_p$ by the scalar field of the elastic modulus G_{eq}:

$$\boldsymbol{\gamma}_e(\mathbf{x}) - \boldsymbol{\gamma}_{e,n}(\mathbf{x}) = \frac{\boldsymbol{\tau}_p(\mathbf{x})}{G_{eq}(\mathbf{x})} \tag{14}$$

where $\boldsymbol{\gamma}_e - \boldsymbol{\gamma}_{e,n}$ is the elastic strain measured with respect to the neutral configuration $\boldsymbol{\gamma}_{e,n}$ – the configuration that the material in its present microstructural state would eventually acquire if the stress were set to zero (for further details, De Souza Mendes, 2009). The interest is on the intensity of $\boldsymbol{\gamma}_e - \boldsymbol{\gamma}_{e,n}$, denoted by $\Delta\gamma_e$ and defined as

$$\Delta\gamma_e = \sqrt{\frac{1}{2}\mathrm{tr}(\boldsymbol{\gamma}_e - \boldsymbol{\gamma}_{e,n})^2} = \frac{1}{G_{eq}}\sqrt{\frac{1}{2}\mathrm{tr}\,\boldsymbol{\tau}_p^2} = \frac{\tau_p}{G_{eq}} \tag{15}$$

The influence of the material elasticity in the morphology of the flow unyielded regions and on the elastic strain field is shown in Fig. 3, for $\rho^* = 0$, $J = 5 \times 10^3$, $n = 0.5$ and $U^* = 0.1$, with θ_0^* equal to 0.75 and 25. For the higher value of the microstructure shear modulus ($\theta_0^* = 25$) the unyielded zones (the black ones in figures) are almost fore-aft symmetric in the absence of inertia and elasticity effects and the elastic strain in the cavity is essentially negligible. For ($\theta_0^* = 0.75$), in addition to the tilting of the cavity unyielded region, it is observed the highest elastic strains occuring in regions where the ratios of stress to stiffness are highest – what happens when the material is still highly structured and the stress is in the vicinity of the yield stress (highest possible stress while the material is highly structured).
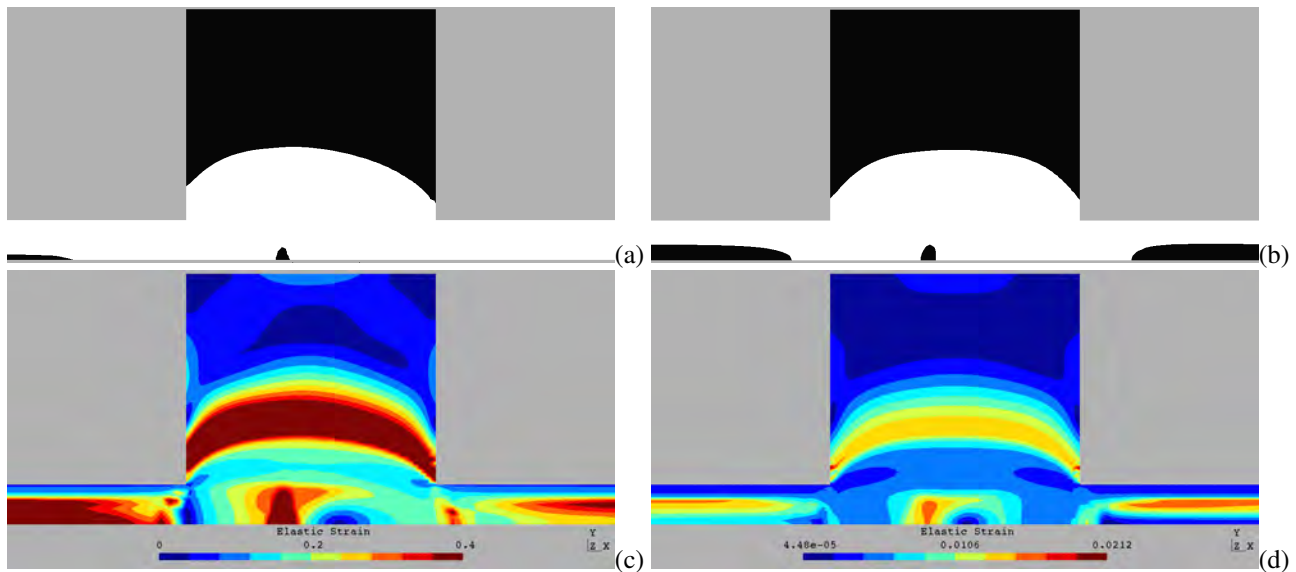

Figure 3. Effect of the elasticity on the flow, for $\rho^* = 0$, $U^* = 0.1$, $J = 5 \times 10^3$ and $n = 0.5$ – Yielded and unyielded regions for (a) $\theta_0^* = 0.75$ and (b) $\theta_0^* = 25$; elastic strain for (c) $\theta_0^* = 0.75$ and (d) $\theta_0^* = 25$.

Figure 4 show the effects of the dimensionless flow rate on the unyielded regions and elastic strain field for $\rho^* = 0$, $J = 5 \times 10^3$, $n = 0.5$ and $\theta_0^* = 1.0$, with U^* equal to 0.01 and 1.0. Large elastic strains occur throughout the flow domain for the smaller value of U^*, while are reduced for $U^* = 1.0$. This behavior is observed due to the higher stress levels induced increasing the flow rate, which implies low structuring levels and hence high G_{eq}. The same reasoning can be used to explain the trend observed for the unyielded regions, decreasing monotonically as the dimensionless inlet velocity is increased.

The effect of inertia is illustrated on Fig. 5 for $\theta_0^* = 1.0$, $J = 5 \times 10^3$, $U^* = 0.1$ and $n = 0.5$, with $\rho^* = 1.0$ and (b) $\rho^* = 500$. The elastic strain field suffers minor effects of inertia once, for a fixed microstructure shear modulus, the dimensionless inlet velocity remains unchanged. Due to the type of scaling employed in this work (De Souza Mendes, 2007), the changes on the flow field entailed by inertia are decoupled from the changes entailed by the imposed changes in the flow intensity. The shape of the cavity yield surface, however, changes significantly in the presence of inertial effects: while elasticity tends to tilt this yield surface counter-clockwise, inertia has the opposite effect. The cavity yield surface shown for $\rho^* = 500$ is tilted clockwise, despite the high level of elasticity.

D. Santos, G. Furtado, S. Frey, M. Naccache, P. de Souza Mendes
Numerical Investigation Of Elastic And Viscous Effects On Inertial Viscoplastic Fluid Flows
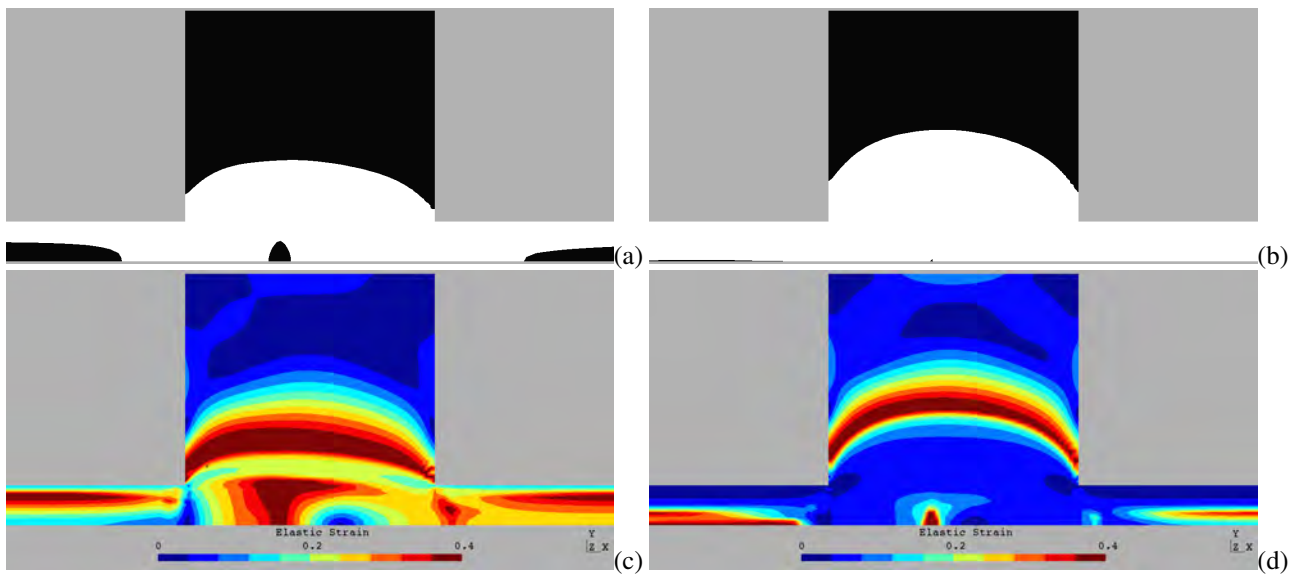

Figure 4. Effect of the dimensionless flow rate on the flow, for $\rho^* = 0$, $\theta_0^* = 1.0$, $J = 5 \times 10^3$ and $n = 0.5$ – Yielded and unyielded regions for (a) $U^* = 0.01$ and (b) $U^* = 1.0$; elastic strain for (c) $U^* = 0.01$ and (d) $U^* = 1.0$.
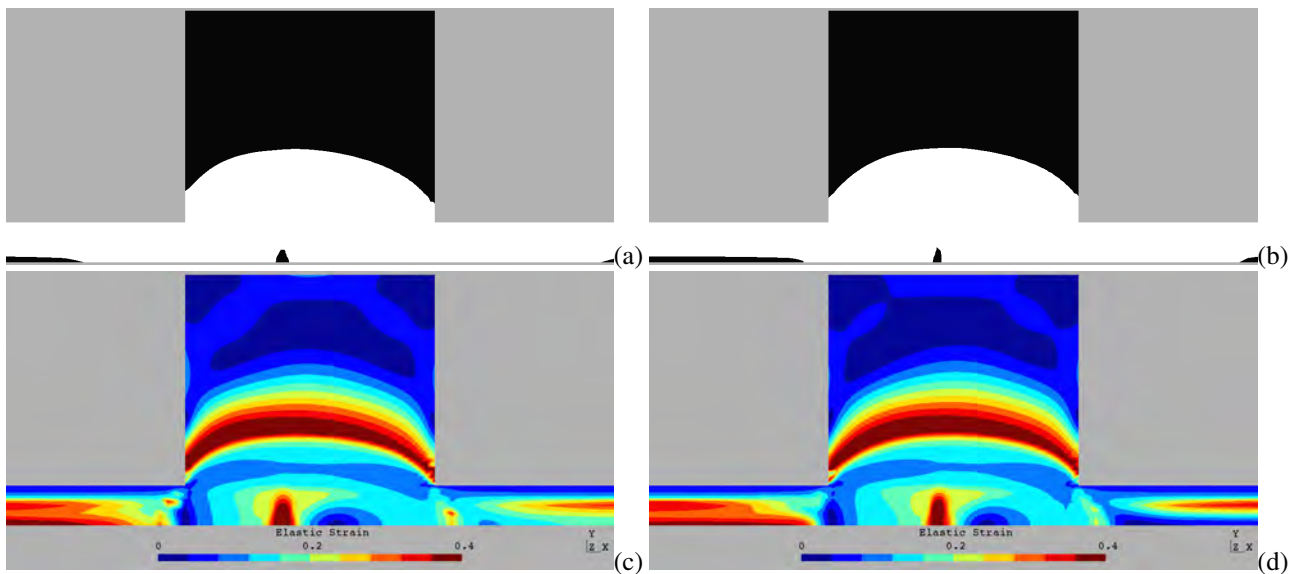

Figure 5. Effect of the inertia on the flow, for $\theta_0^* = 1.0$, $J = 5 \times 10^3$, $U^* = 0.1$ and $n = 0.5$ – Yielded and unyielded regions for (a) $\rho^* = 1.0$ and (b) $\rho^* = 500$; elastic strain for (c) $\rho^* = 1.0$ and (d) $\rho^* = 500$.

5. FINAL REMARKS

In this article, some numerical simulations of inertial flows of elasto-viscoplastic fluids have been undertook. The elasto-viscoplastic model was based on the Oldroyd-B viscoelastic equation and the mechanical model was approximated via a multi-field Galerkin least-squares method in extra-stress, pressure and velocity. Due to the good stability features of the GLS method, all computations have employed a combination of equal-order bilinear Lagrangian finite elements and high elastic flows have been stably achieved. The numerical results have evidenced the strong influence of the microstructure shear modulus and inertia on the position of the unyielded material regions. Also the yield stress level – variated via the flow intensity U^* – proved to play a relevant role on the characterization of the unyielded zones.

6. ACKNOWLEDGEMENTS

7. REFERENCES

Behr, A.M., Franca, L.P., Tezduyar, T.E., 1993. "Stabilized finite element methods for the velocity–pressure–stress formulation of incompressible flows", Computer Methods in Applied Mechanics and Engineering, vol. 104, pp. 31-48.

Beverly, C.R., Tanner, R.I., 1989. "Numerical analysis of extrudate swell in viscoelastic materials with yield stress", Journal of Rheology, vol 33 (6), pp. 989-1009.

Carter, R.E., Warren, R.C., 1987. "Extrusion stresses, die swell, and viscous heating effects in double-based propellants", Journal of Rheology, vol 31, pp. 151-173.

De Souza Mendes, P.R., Dutra, E.S.S., 2004. "Viscosity Function for Yield-Stress Liquids", Applied Rheology, vol. 14, pp. 296-302.

De Souza Mendes, P.R., 2007. "Dimensionless non-Newtonian fluid mechanics", Journal of Non-Newtonian Fluid Mechanics, vol. 147, pp. 109-116.

De Souza Mendes, P.R., Naccache, M.F., Varges, P.R., Marchesini, F.H., 2007. "Flow of viscoplastic liquids through axisymmetric expansions-contractions", Journal of Non-Newtonian Fluid Mechanics, vol. 142, pp. 207-217.

De Souza Mendes, P.R., 2009. "Modeling the thixotropic behavior of structured fluids", Journal of Non-Newtonian Fluid Mechanics, vol. 164, pp. 66-75.

Franca, L.P., Frey, S.L., 1992. "Stabilized finite element methods: II. The incompressible Navier-Stokes equations", Computer Methods in Applied Mechanics and Engineering, vol. 99, pp. 209-233.

Hughes, T.J.R., Franca, L.P., Balestra, M., 1986. "A new finite element formulation for computational fluid dynamics: V. Circumventing the Babuška-Brezzi condition: A stable Petrov-Galerkin formulation of the Stokes problem accommodating equal-order interpolations", Computer Methods in Applied Mechanics and Engineering, vol. 59, pp. 85-99.

Matallah, H., Townsend, P., Webster, M.F., 1998. "Recovery and stress-splitting schemes for viscoelastic flows", Journal of Non-Newtonian Fluid Mechanics, vol. 75, pp. 139-166.

Mujumdar, A., Beris, A.N., Metzner, A.B., 2002. "Transient phenomena in thixotropic systems", Journal of Non-Newtonian Fluid Mechanics, vol 102, pp. 157-178.

Santos, D.D., Frey, S.L., Naccache, M.F., de Souza Mendes, P.R., 2011. "Numerical approximations for flow of viscoplastic fluids in a lid-driven cavity", Journal of Non-Newtonian Fluid Mechanics , vol. 166, pp. 667-679.

Sikorski, D., Tabuteau, H., de Bruyn, J.R., 2009. "Motion and shape of bubbles rising through a yield-stress fluid", Journal of Non-Newtonian Fluid Mechanics, vol 159, pp. 10-16.

8. RESPONSIBILITY NOTICE